

THE TIMING AND DIRECTIONAL CONNECTIVITY OF HUMAN FRONTOPARIETAL AND VENTRAL VISUAL ATTENTION NETWORKS IN EMOTIONAL SCENE PERCEPTION

D. SABATINELLI,^{a*} D. W. FRANK,^a T. J. WANGER,^a
M. DHAMALA,^b B. M. ADHIKARI^b AND X. LI^c

^a Department of Psychology & Neuroscience, Biolumaging Research Center, University of Georgia, Athens, GA 30602, United States

^b Department of Physics & Astronomy, Neuroscience Institute, Center for Behavioral Neuroscience, Georgia State University, Atlanta, GA 30302, United States

^c Department of Computer Science, Biolumaging Research Center, University of Georgia, Athens, GA 30602, United States

Abstract—Electrocortical and hemodynamic measures reliably identify enhanced activity in the ventral and dorsal visual cortices during the perception of emotionally arousing versus neutral images, an effect that may reflect directive feedback from the subcortical amygdala. However, other brain regions strongly modulate visual attention, such as frontal eye fields (FEF) and intraparietal sulcus (IPS). Here we employ rapid sampling of BOLD signal (4 Hz) in the amygdala, fusiform gyrus (FG), FEF and IPS in 42 human participants as they viewed a series of emotional and neutral natural scene photographs balanced for luminosity and complexity, to test whether emotional discrimination is evident in dorsal structures prior to such discrimination in the amygdala and FG. Granger causality analyses were used to assess directional connectivity within dorsal and ventral networks. Results demonstrate emotionally-enhanced peak BOLD signal in the amygdala, FG, FEF, and IPS, with the onset of BOLD signal discrimination occurring between 2 and 3 s after stimulus onset in ventral structures, and between 4 and 5 s in FEF and IPS. Granger causality estimates yield stronger directional connectivity from IPS to FEF than the reverse in this emotional picture paradigm. Consistent with a reentrant perspective of emotional scene perception, greater directional connectivity was found from the amygdala to FG compared to the reverse. These data support a perspective in which the registration of emotional scene content is orchestrated by the amygdala and rostral inferotemporal visual cortex. © 2014 IBRO. Published by Elsevier Ltd. All rights reserved.

Key words: emotion, attention, scene perception, human.

INTRODUCTION

Electrocortical and hemodynamic measures reveal enhanced activity in ventral and dorsal visual cortices during emotional relative to neutral picture perception (Pourtois et al., 2004; Sabatinelli et al., 2005; Pessoa et al., 2006; Anticevic et al., 2011; Sabatinelli et al., 2013; Wiens and Syryjanen, 2013), an effect that may reflect a natural selective attention to behaviorally relevant stimuli (Vuilleumier and Driver, 2007; Lang and Bradley, 2010; Pessoa and Adolphs, 2010; Markovic et al., 2013). Some evidence suggests an association between enhanced fusiform gyrus (FG) activity and directive feedback from the subcortical amygdala (Armony and Dolan, 2002; Vuilleumier et al., 2004; Sabatinelli et al., 2005, 2009).

However, other brain regions strongly modulate visual attention, such as frontal eye fields (FEF) and intraparietal sulcus (IPS) (Rizzolatti et al., 1987; Corbetta, 1998; Schafer and Moore, 2007; Bisley and Goldberg, 2010). This frontoparietal (FP) network is persistently involved in a process of categorizing stimulus relevance and directing the locus of visual attention (Corbetta et al., 2008). While the characteristics of this FP network have been thoroughly investigated in target-driven visuospatial attention tasks (Serences and Yantis, 2006) the role of stimulus emotion on the engagement of this network is underexplored. While studies have demonstrated that emotional stimuli evoke augmented FP activity (Moratti et al., 2004; Sabatinelli et al., 2007a,b; Shafer and Dolcos, 2012; Brosch and Grandjean, 2013; Ferri et al., 2013), the mechanisms by which emotional characteristics modulate FP activity are poorly defined (Adolphs, 2002; Mitchell et al., 2008; Vuilleumier and Huang, 2009; Frank and Sabatinelli, 2012).

One means of addressing research questions regarding the temporal order of human brain activity is through comparisons of the relative timing of the BOLD signal within a structure across experimental conditions. While the BOLD signal is inherently delayed and smoothed relative to neural activity, the timing of signal change within active clusters is highly reliable (Kim et al., 1997; Menon and Kim, 1999; Miezin et al., 2000; Lin et al., 2013). Here we sample the BOLD contrast four times per second in 4-slice slabs of ventral (amygdala and FG) and dorsal (FEF and IPS) brain regions during an

*Corresponding author. Address: 523 Psychology, University of Georgia, Athens, GA 30602, United States.

E-mail address: sabat@uga.edu (D. Sabatinelli).

Abbreviations: ANOVA, analysis of variance; FEF, frontal eye fields; FG, fusiform gyrus; fMRI, functional magnetic resonance imaging; FP, frontoparietal; GC, Granger causality; IAPS, International Affective Picture System; IPS, intraparietal sulcus; ROI, region of interest; TR, repeat time.

emotional and neutral picture series to test whether emotional discrimination is apparent in the FP network prior to such emotional discrimination in the amygdala and FG. There is evidence for a rapid response latency in human (Kirchner et al., 2009) and macaque (Schmoelesky et al., 1998) FEF, and human data that suggest a role for FEF in modulating attention enhancement in the visual cortex (Taylor et al., 2007). If picture stimulus emotion is discriminated in the FP network prior to the amygdala and FG, a reentrant perspective of emotional perception (Freese and Amaral, 2005; Sabatinelli et al., 2009; Vuilleumier and Huang, 2009) would not be supported. If emotional discrimination is apparent in the amygdala and FG prior to such discrimination in the FP network, the emotionally-enhanced activity seen in FP structures during scene perception may reflect input from the amygdala and FG, or other regions not yet sampled.

Rapid sampling also provides an opportunity to determine potential asymmetries in directional connectivity between structures within the ventral and dorsal networks using Granger connectivity analyses. As there is support for a directive effect of the amygdala on FG (Anderson and Phelps, 2001; Vuilleumier and Driver, 2007; Sabatinelli et al., 2009) and for the FEF on IPS (Bressler et al., 2008), the current data will enable a test of these hypothesized directional connectivities in an emotional picture perception task.

EXPERIMENTAL PROCEDURES

Participants and procedure

Forty-five undergraduate students from the University of Georgia participated in the experiment, receiving \$20 USD compensation. Three subjects' data were lost due to MR scanner or stimulus presentation equipment malfunction. Of the 42 participants (average age 22 years, standard deviation (SD) 3) in the final sample, 20 were female. All participants gave informed consent, and this study was approved by the University of Georgia Human Subjects Review Board. All participants reported no neurological abnormalities and had normal or corrected-to-normal vision. Participants were given instructions and provided ratings of pleasantness and emotional arousal of the experimental picture stimuli, printed in booklet form. Prior to entering the bore of the scanner, participants were fitted with earplugs, headphones, fiber-optic goggles (Resonance Technology, Inc., San Diego, CA, United States) and given a patient-alarm squeeze ball. Padding inside the head coil and explicit verbal instruction were used to limit head motion. Each participant spent approximately 45 min inside the scanner, during which they received a structural scan and a series of functional scans. In each functional scan, participants were instructed to attend to each picture and maintain fixation on a red point at the center of the screen throughout the picture series.

Stimuli

Participants viewed a pseudo-randomly ordered series of pleasant, neutral and unpleasant pictures presented in

256 levels of grayscale, at 800×600 resolution, over a 30° horizontal field of view. The picture stimuli depicted categories of content including (1) erotic couples, (2) romantic couples and happy children/families, (3) land/city scapes and people in daily activities, (4) threatening animal and people, and (5) scenes of graphic bodily injury. All stimuli were balanced by category to be statistically equivalent in luminosity using GIMP 2.8 (www.gimp.org). Each participant was presented with four blocks of 20 pictures, with the functional prescription shifting across blocks (described further below). Sixty of the 80 (20 stimuli were omitted due to a computational error) pictures used in the experiment were balanced to be statistically equivalent in joint photographic experts group (JPEG) file size at 90% quality, as a rough gauge of visual complexity. Each picture block began with a 2-s checkerboard acclimation image, followed by a series of 20 experimental picture stimuli presented for 2 s each, interspersed with fixation-only periods of 9–11 s.

Scanning parameters

Once participants were situated inside the magnet, a T1-weighted structural volume was collected consisting of 156 sagittal slices with a 256×256 matrix and 1-mm isotropic voxels. The functional prescriptions were each comprised of four oblique axial slices (64×64 gradient echo planar imaging (EPI), 18-cm field of view (FOV), 5-mm thickness, 1-mm gap, 25° flip angle, 30-ms echo time (TE), 250-ms repeat time (TR)) positioned over slabs of the brain to enable coverage of the amygdala, FG, and substantial regions of calcarine fissure in one prescription, and IPS and FEF in another. The order of prescription sampling was counterbalanced across participants. Each set of four slices was manually positioned using the T1 volume for visual identification of landmarks based on each participant's anatomy. As depicted in Fig. 1, a 4-slice prescription over the amygdala and FG was centered on the amygdala and tilted to abut the border between the ventral temporal lobe and cerebellum. The 4-slice prescription covering IPS and FEF was centered on the IPS and tilted to cover the superior frontal lobe, using cluster locations functionally derived from prior work as a guide (Paus, 1996; Sabatinelli et al., 2007a; Shafer and Dolcos, 2012). Two additional slice prescriptions were acquired but are not presented here.

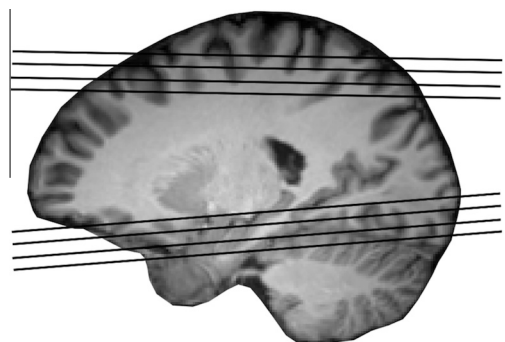


Fig. 1. The approximate location of the 4-slice, 250-ms TR functional prescriptions described in this study.

Image processing and analyses

Each functional time series was motion corrected using trilinear interpolation, spatially smoothed across two voxels (5.625 mm full width at half maximum), linearly de-trended and filtered at 0.02-Hz high pass, and temporally smoothed with a 3-point (750 ms) Gaussian filter using BrainVoyager QX 2.8 (Brain Innovation; brainvoyager.com). Great care was taken at acquisition to limit head motion, with explicit verbal instruction and extensive head padding. In post-processing, trials with residual motion were removed manually, by identifying large (greater than four times the background variation) and brief spikes in the time series that are indicative of head motion. These spikes were located by examining the average signal intensity across a majority of the voxels in a slice (a rectangular region of greater than half the voxels within the brain). This procedure resulted in the removal of less than 2% of total trials, and no more than four trials from any subject. Single-subject analysis of variances (ANOVAs) were then performed on the time-series data to identify the BOLD signal associated with picture presentations. A two-gamma hemodynamic response function was employed (Friston et al., 1998), and a false discovery rate of $p < 0.05$ (Genovese et al., 2002) was applied to control for multiple comparisons. A 10-mm³ cluster of activity was sampled from significantly active voxels in each region of interest (ROI). The coordinates for these functionally active clusters were guided a priori by locations observed in previous studies of emotional picture perception (Liu et al., 2012; Sabatinelli et al., 2011; Sabatinelli et al., 2013) and visual attention in IPS and FEF (Dyckman et al., 2007; Sabatinelli et al., 2007a; Shafer and Dolcos, 2012). Percent signal change at peak (deviated from pre-trial baseline) was calculated using the average BOLD signal from 3 to 9-s post stimulus onset.

Time series discrimination across stimulus content

To reliably identify the point at which emotion-specific BOLD signal increases occurred in the amygdala, FG, calcarine fissure, IPS, and FEF, non-parametric permutation tests (Maris, 2004; Maris and Oostenveld, 2007) were computed for each time point and region in the first 6 s (24 time points) of picture presentation. Labels encoding picture valence (pleasant, neutral, and unpleasant) were randomly reassigned in 5000 draws, and checked for independence from previous permutation orders. A repeated measures F -statistic was then generated for each time point, and a Gaussian function fit to the distribution. The value of the F -statistic used in forming the permutation distribution was computed as the 99.5th percentile of the distribution described by this fitted Gaussian ($p < .05$). Correction for multiple comparisons was achieved at a cluster threshold of three successive time points (Maris and Oostenveld, 2007).

Granger causality (GC) analyses

The time series of each pair of ROIs (amygdala & FG, IPS & FEF) from all participants were segmented into epochs

(trials) based on the onset times of the stimuli. After removing the stimulus-triggered ensemble average from each trial waveform, the resulting trials from all participants were entered into GC spectral analysis (Geweke, 1982; Ding et al., 2006) to identify the overall frequency, degree, and direction of causal influences between the ROIs. GC spectra can be estimated by parametric and nonparametric methods (Dhamala et al., 2008). GC spectra from the parametric and nonparametric match very well when many data samples are collected and appropriately modeled in the parametric approach. In practice, we have a limited number of data points, even when sampling at 4 Hz, but we still need to find an appropriate model order. As it is often difficult to find an appropriate model order for brain data with the traditional akaike information criterion (AIC) and Bayesian information criterion (BIC) criteria (Dhamala et al., NeuroImage, 2008; Antzoulatos and Miller, 2014), when appropriately modeled, the parametric method yields GC values that have no bias or less bias for short time series data (please see the appendix of Dhamala et al., NeuroImage, 2008). To take advantage of both approaches, here we determined the optimal model order for the parametric method using a method developed recently (Adhikari et al., 2014) by comparing the power spectra from the nonparametric and parametric approaches at different model orders, and choosing the model order yielding the lowest power difference. The spectral GC from ROI l to ROI m is defined as (Ding et al., 2006; Dhamala et al., 2008):

$$l_{l \rightarrow m} = \ln \frac{S_{mm}}{S_{mm} - |H_{lm}|^2 \left(\sum_{ll} - \frac{\Sigma_{lm}^2}{\Sigma_{mm}} \right)} \quad (1)$$

where S is power spectra, H is transfer function, and noise covariance Σ .

The significant peaks in the GC spectra were defined by setting a GC threshold above the random-noise baseline at significance $p < .001$. To find this threshold, we computed GC from 1000 surrogate data sets that were constructed by randomly shuffling trials across ROIs and participants, and evaluated the distribution of maximum GC values (Dhamala et al., 2008). The threshold was thus based on the null hypothesis that there was no statistical interdependence between nodes when trials were randomized. After identifying significant peaks in the causality spectra, the causality spectra within the frequency band of interest were integrated over the frequency band to compute the overall band-specific GC:

$$F_{l \rightarrow m} = \frac{1}{f_2 - f_1} \int_{f_1}^{f_2} l_{l \rightarrow m}(f) df, \quad (2)$$

where $f_2 - f_1$ is the frequency interval (band) of interest.

RESULTS

Stimulus ratings

Averages and standard errors of valence and arousal ratings for the 80 picture stimuli used in this study are shown in Table 1. The ratings for the 20 picture stimuli selected from the International Affective Picture System (IAPS) are drawn from the normative values (also drawn

Table 1. Picture stimulus ratings

		Pleasant	Neutral	Unpleasant
Ratings of 20 IAPS stimuli	Valence	7.14 (.16)	5.88 (.45)	2.89 (.30)
	Arousal	5.65 (.32)	3.71 (.28)	6.34 (.27)
Ratings of 60 picture stimuli	Valence	6.93 (.18)	5.89 (.16)	2.87 (.20)
	Arousal	6.03 (.14)	3.65 (.22)	6.71 (.16)

Average (standard error) of self-reported valence and arousal ratings for the 80 picture stimuli used in this study. Ratings for the 20 picture stimuli used in Study 1 are drawn from IAPS normative values (Lang et al., 2008).

from undergraduate sample) published in the IAPS technical manual (Lang et al., 2008), and differed reliably across valence ($F(2, 17) = 69.00, p < .001$) with pleasant stimuli yielding higher valence ratings relative to neutral stimuli ($F(1, 10) = 10.89, p < .01$), which yielded higher valence ratings relative to unpleasant stimuli ($F(1, 10) = 30.80, p < .001$). Ratings of emotional arousal were also reliably different across pleasant, neutral, and unpleasant stimuli ($F(2, 17) = 14.70, p < .001$) with neutral stimuli yielding lesser ratings of emotional arousal relative to pleasant ($F(1, 10) = 14.92, p < .01$) and unpleasant stimuli ($F(1, 10) = 37.18, p < .001$), with unpleasant stimuli equivalent arousal ratings relative to pleasant stimuli ($F(1, 14) = 2.69, p > .1$). The remaining 60 pictures (assembled by our lab to be consistent with the IAPS stimuli) were rated equivalently by 26 participants, and differed reliably across valence ($F(2, 50) = 115.68, p < .001$) with pleasant stimuli yielding higher valence ratings relative to neutral stimuli ($F(1, 25) = 34.28, p < .001$), which yielded higher valence ratings relative to unpleasant stimuli ($F(1, 25) = 96.54, p < .001$). Ratings of emotional arousal were also reliably different across pleasant, neutral, and unpleasant stimuli ($F(2, 50) = 83.29, p < .001$) with neutral stimuli yielding lesser ratings of emotional arousal relative to pleasant ($F(1, 25) = 86.16, p < .001$) and unpleasant stimuli ($F(1, 25) = 106.98, p < .001$), with unpleasant stimuli prompting greater arousal ratings relative to pleasant stimuli (6.71 vs. 6.03 on a 1–9 scale; $F(1, 25) = 14.30, p < .01$).

Picture-driven activation in regions of interest

Fig. 2 represents the random-effects ANOVA output of dorsal (2A) and ventral (2B) regions thresholded at a false discovery rate of $p < .01$, overlaid on the averaged standardized structural volume of the participant sample, and, for comparison, Fig. 3 represents the activity of a single subject. Table 2 presents the number of participants contributing, location, size, and statistical reliability of the regions of interest sampled in the study. Peak scores (BOLD signal change from 3 to 9 s after, deviated from the 250 ms prior to picture onset) were averaged by subject and ROI, and tested with multivariate ANOVA including hemisphere and picture content as factors. We used Wilks' lambda to assess whether the individually-extracted peak BOLD signal change values from the four ROIs were reliably different across picture contents. No interactions with the hemisphere were significant, and thus scores from bilateral ROIs were averaged and the analyses were recalculated. Shown in Table 3, peak

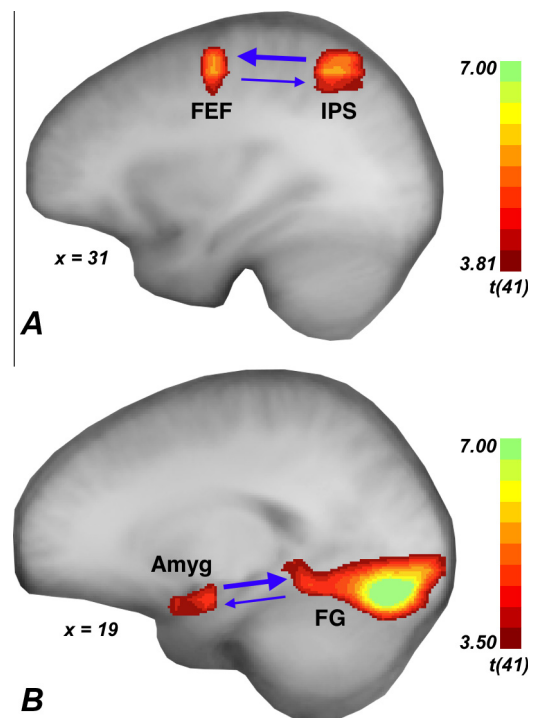


Fig. 2. The random-effects group average of picture-driven activation in dorsal (A) and ventral (B) regions, thresholded at $FDR < .01$, overlaid on the average of standardized structural volumes from the sample. Blue arrows indicate significant bidirectional Granger causality values between FEF and IPS (A) and the amygdala and FG (B). Heavy arrows indicate significantly greater directional connectivity from the amygdala to FG, and from IPS to FEF. (For interpretation of the references to color in this figure legend, the reader is referred to the web version of this article.)

BOLD signal change across the amygdala, FG, FEF and IPS showed significant effects of picture valence, and followed a quadratic trend, indicating greater BOLD signal change during pleasant and unpleasant, relative to neutral picture presentation. No linear effects were significant. Picture valence had no effect on BOLD signal change in the calcarine fissure.

Timing of BOLD signal change across picture contents

Fig. 4 shows the time course of the BOLD signal change across pleasant, neutral, and unpleasant picture presentations. The point of reliable BOLD signal enhancement during emotional, relative to neutral pictures is indicated by the arrow along the x-axis of time, and yielded onsets of 2.25 s for the amygdala,

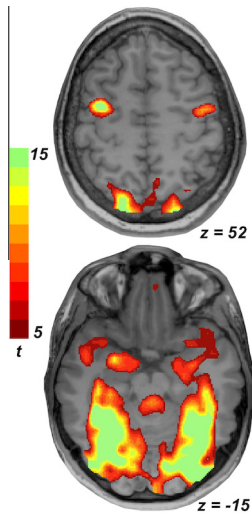


Fig. 3. An overlay of significant picture-driven functional activity from a single participant in dorsal (top) and ventral (bottom) prescriptions, depicting bilateral activity in frontal eye fields, intraparietal sulcus, amygdala, and ventral visual structures.

2.5 s for FG, 4.25 s for IPS, and 4.75 s for FEF. Illustrated another way, a plot of the alpha value representing reliable picture valence discrimination for each ROI is shown in Fig. 5, focusing on the period from 2 to 6 s after picture onset. Interactions representing significantly delayed emotional discrimination in dorsal versus ventral structures did not reach significance. Fig. 6 demonstrates the consistency of BOLD signal timing across dorsal and ventral regions across all stimulus conditions.

Directional connectivity analyses

GC analyses over a .09–1.8-Hz frequency band were used to estimate the strength of directional connectivity between the amygdala and FG, and between IPS and FEF for each participant across the stimulus series. One subject with GC values six standard deviations above the mean was excluded from the ventral ROI analysis. As shown in Fig. 7, the amygdala and FG showed a significant bidirectional influence ($p < .001$ threshold at $GC > .0144$), with the amygdala showing greater directional connectivity to FG relative to the reverse ($F(1, 40) = 7.37, p < .01$). The FEF and IPS also showed significant bidirectional influence ($p < .001$ threshold at $GC > .0120$), with IPS showing greater directional connectivity to FEF relative to the reverse ($F(1, 40) = 14.76, p < .001$). These GC results are also represented as heavy or light arrows between ROIs in Fig. 2.

DISCUSSION

Assessing the relative contributions of dorsal and ventral structures to the process of emotional discrimination in humans is methodologically challenging, as high levels of spatial and temporal resolution are necessary, and direct access to all structures of interest via invasive methods is extremely rare. Moreover, ventromedial cortical and subcortical regions present a particularly weak signature in the noninvasive electro- and magneto-encephalogram. One means of addressing the research problem is achievable through tracking the relative timing of the BOLD signal within a structure across emotional relative to neutral stimulus processing

Table 2. Region of interest location, size, and t -statistic of picture-driven activation

ROI	N	Left					Right				
		x	y	z	Vol	t	x	y	z	Vol	t
Amygdala	39	-20.0 (.8)	-6.1 (.6)	-15.1 (.6)	712 (41)	5.0 (.4)	18.4 (.7)	-6.2 (.6)	-14.9 (.7)	705 (44)	5.4 (.5)
Fusiform gyrus	42	-33.2 (.8)	-44.6 (.9)	-14.0 (.8)	941 (16)	10.2 (.7)	26.7 (.8)	-43.2 (1.0)	-13.8 (.7)	939 (20)	11.4 (.9)
Intraparietal sulcus	40	-27.9 (1.7)	-58.7 (.8)	54.7 (.7)	938 (19)	8.8 (.7)	29.0 (.6)	-58.2 (.8)	54.6 (.6)	900 (20)	8.6 (.7)
Frontal eye fields	41	-44.0 (.6)	-6.3 (.8)	52.4 (.8)	906 (21)	7.8 (.6)	44.4 (.5)	-3.8 (.6)	54.3 (1.8)	880 (30)	8.1 (.6)
Calcarine fissure	42	-3.7 (.5)	-90.4 (.6)	-8.1 (1.0)	927 (14)	13.1 (.9)					

Means and standard errors of the location in Talairach space (Talairach and Tournoux, 1988), volume (in μl) and t -statistic for bilateral regions of interest (ROI) sampled in the study. The midline calcarine fissure ROI is listed in the left column. The number of subjects (of 42 total) contributing to the ROI is listed in column N . All ROIs were sampled from voxels significantly activated ($FDR < .05$) by the onset of a picture stimulus. T -statistic values represent the average of all voxels within the cluster. The minimum cluster size (across both left and right ROI) is 250 μl , and the maximum volume for each left and right ROI sample is a 1000 μl cube.

Table 3. Region of interest peak BOLD percent signal change effects across picture contents

ROI	Pleasant	Neutral	Unpleasant	Valence F, p	Quadratic F, p	Linear F, p
Amygdala	.140 (.04)	.031 (.03)	.153 (.02)	(2,37) = 4.32, $p < .05$	(1,38) = 8.03, $p < .01$	(1,38) = .080, ns
Fusiform gyrus	.307 (.03)	.225 (.04)	.312 (.03)	(2,40) = 4.09, $p < .05$	(1,41) = 7.95, $p < .05$	(1,41) = .032, ns
Intraparietal sulcus	.293 (.03)	.131 (.04)	.278 (.04)	(2,38) = 5.05, $p < .05$	(1,39) = 10.37, $p < .01$	(1,39) = .164, ns
Frontal eye fields	.284 (.03)	.106 (.06)	.233 (.03)	(2,39) = 3.85, $p < .05$	(1,40) = 5.09, $p < .05$	(1,40) = 3.20, ns
Calcarine fissure	.820 (.11)	.838 (.10)	.836 (.10)	(2,40) < 1, ns	(1,41) < 1, ns	(1,41) < 1, ns

Means and standard errors of peak BOLD signal change, F -statistic, p -value, and trend tests in the regions of interest sampled in this study across pleasant, neutral, and unpleasant picture contents.

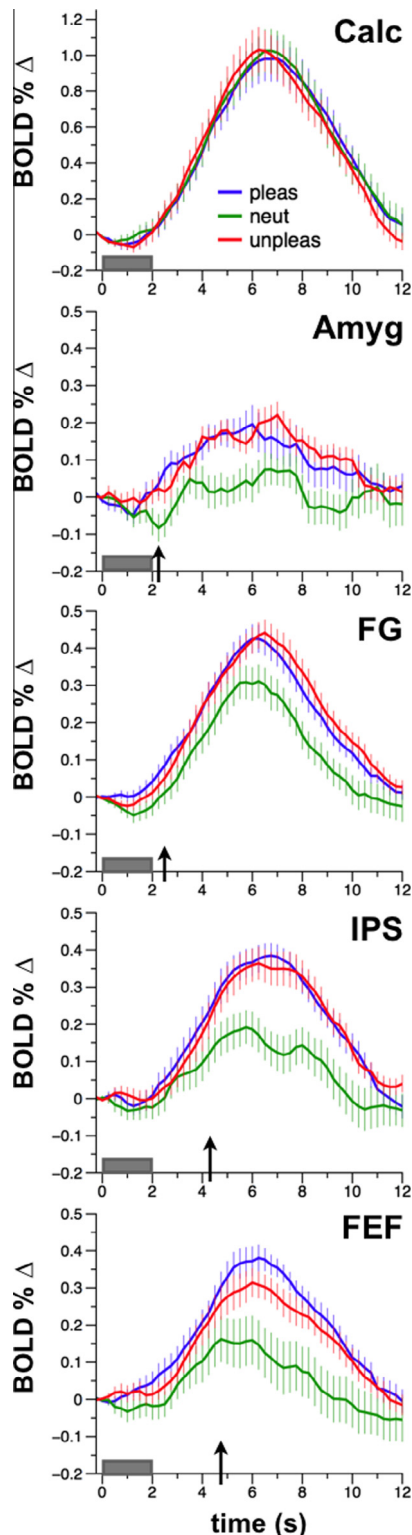


Fig. 4. The time course of the BOLD signal in percent change, deviated from a pre-picture baseline of 250 ms in calcarine fissure (calc), amygdala (Amyg), fusiform gyrus (FG), intraparietal sulcus (IPS) and frontal eye fields (FEF) across pleasant (blue), neutral (green) and unpleasant (red) picture contents. Along the abscissa, the gray bar represents the picture stimulus duration, and arrows indicate the time point at which reliable emotional discrimination occurred in the structure. (For interpretation of the references to colour in this figure legend, the reader is referred to the web version of this article.)

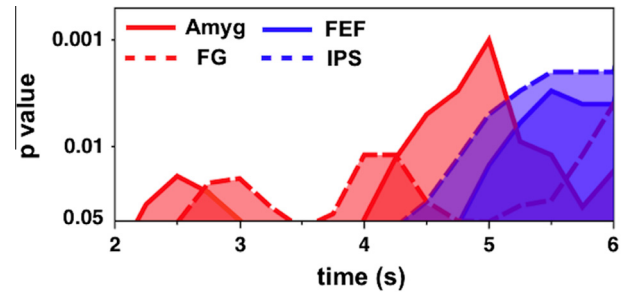


Fig. 5. The onset of reliable discrimination of emotional picture content within the ventral (red) and dorsal (blue) regions of interest, expressed as a *p*-value. (For interpretation of the references to colour in this figure legend, the reader is referred to the web version of this article.)

using rapid sampling in focused regions of interest. While the BOLD signal is inherently delayed and smoothed relative to neural activity, the timing of signal change within active clusters is highly reliable (Kim et al., 1997; Menon and Kim 1999; Miezin et al., 2000; Lin et al., 2013). By comparing the time course of the BOLD signal within regions of interest across experimental conditions, the effective temporal resolution is limited only by the sampling rate at which the BOLD signal can be reliably recorded. With each region serving as its own timing control, potential confounds regarding variations in vascular anatomy, as well as individual differences in BOLD timing (Aguirre et al., 1998; Buxton et al., 1998), can be avoided. Considering the strong relationship between local field potentials and the BOLD signal (Logothetis and Wandell, 2004), we may reasonably interpret the time-resolved BOLD signal as representing underlying neural activity of interest. The current rapid-sampling technique has been employed to sample the amygdala and ventral visual cortex during emotional and nonemotional picture perception, providing support for an amygdalofugal reentrant feedback perspective of visual cortical enhancement during emotional perception (Sabatinelli et al., 2009). This and other efforts to increase the temporal resolution of functional magnetic resonance imaging (fMRI) (Feinberg and Setsompop, 2013) thus have utility to address some basic research questions regarding the timing of neural events.

Consistent with prior studies, BOLD signal from the amygdala and FG recorded in the current study was enhanced during emotionally arousing (pleasant and unpleasant) versus neutral picture perception (Pourtois et al., 2004; Sabatinelli et al., 2005; Pessoa et al., 2006; Anticevic et al., 2011). Sampled at four times per second, the latency at which this emotional-enhanced BOLD signal became significant was 2.25 and 2.5 s after picture onset in the amygdala and FG, consistent with a prior study in which these structures were sampled at 10 times per second (Sabatinelli et al., 2009). Also consistent with prior work, no picture content effects were found in the calcarine fissure, offering some evidence that our efforts to equate the simple physical properties of these complex scene stimuli were successful. The integration of emotional significance into visual perception as a result of recurrent amygdala – FG processing fits well with conceptions of complex scene processing as an iterative,

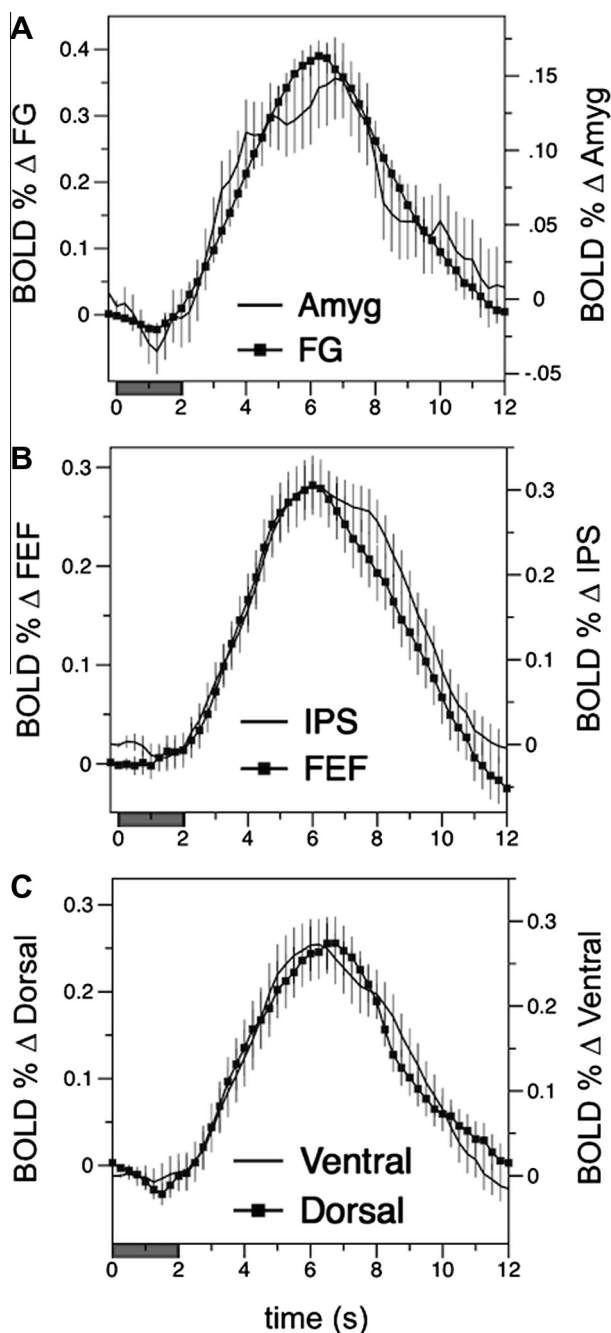


Fig. 6. Double-Y graphs of average BOLD signal change (+ standard errors) across all picture stimuli in the amygdala and FG (A), FEF & IPS (B), and ventral and dorsal ROIs overlaid (C). The picture presentation period is shown as a gray bar from 0 to 2 s along the X axes.

non-hierarchical mechanism (Lamme and Roelfsema, 2000; Grill-Spector and Malach, 2004; Vuilleumier et al., 2005; Hegde and Felleman, 2007; Pessoa and Adolphs, 2010). In the primate, the initial inferotemporal cortical response to a picture of a conspecific is thought to reflect global categorization of the percept, and is followed by a more sustained response that is associated with detail factors such as identity and facial expression (Nakamura et al., 1994; Sugase et al., 1999; Nishijo et al., 2008). The timing of this later stage of detail processing is

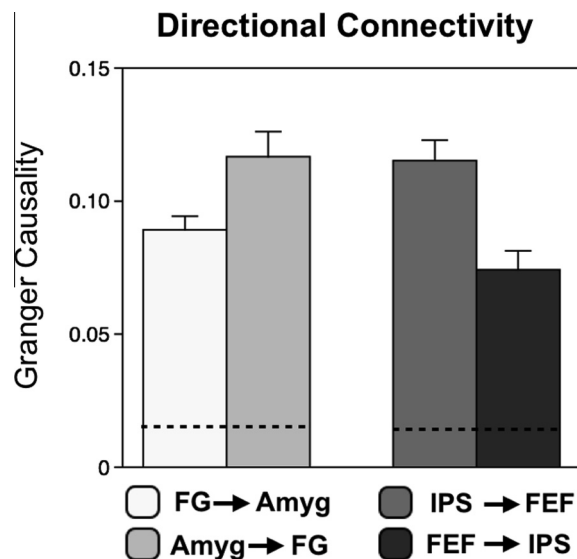


Fig. 7. Granger causality values (+ standard errors) representing directional connectivity across the picture series between the amygdala and FG on the left, and FEF and IPS on the right. The dotted line represents the threshold of significance.

consistent with estimates of scene categorization latency in human research (Junghöfer et al., 2001; VanRullen and Thorpe, 2001; Codispoti et al., 2006; Tsuchiya et al., 2009). We interpret that in the current and previous study (Sabatinelli et al., 2009), this later processing stage underlies the emotionally-enhanced BOLD signal present in the amygdala and FG 2–3 s after stimulus onset. The GC analysis of the interaction between the amygdala and FG in the current study supports the reentrant perspective, in that significantly greater directional connectivity, possibly achieved via the inferior longitudinal fasciculus (Catani et al., 2003), was evident from the amygdala to FG than the reverse.

The FEF and IPS also showed greater activation during emotionally arousing (pleasant and unpleasant) relative to neutral picture perception, consistent with past research using this emotional picture paradigm (Sabatinelli et al., 2007a). This enhancement of the FP network signal was evident despite the fact that picture stimuli were presented across the full visual field, with central fixation, and an instruction to inhibit scanning of the image. While gaze location was not tracked in this study, a previous control experiment employing the same instruction and emotional picture paradigm found no differences in eye movements across pleasant, neutral, and unpleasant picture presentations (Lang et al., 1998). It has also been shown that activity in FEF can be evoked during visual attention tasks in the absence of saccades (Thompson et al., 2005; Armstrong et al., 2009), and thus the presence of significant activity in the current study can be considered relevant to visual attention, and not explicit eye movements. The FEF and IPS are implicated in goal-directed (“top down”) attention and interact with ventral brain areas such as the temporoparietal junction and inferior frontal gyrus, and have been shown to be involved in stimulus-directed attention (Corbetta and Shulman, 2002; Asplund et al., 2010; Carrette, 2014).

The primary aim of this study was to determine whether this dorsal visual attention network demonstrated emotional scene discrimination prior to such discrimination in the amygdala and FG, and these data suggest that this is not the case. In FEF and IPS, the latency of emotionally-enhanced BOLD signal became reliable between 4.25 and 4.75 s after picture onset. Thus, if we accept that the timing of the BOLD signal change within a structure relative to stimulus onset reflects, in part, the role of that structure in stimulus processing (Lin et al., 2013; Miezin et al., 2000), then these data suggest that the FP network activity is unlikely to direct emotional discrimination in the amygdala and ventral visual cortex. Additional work in which dorsal and ventral regions are sampled simultaneously may delineate the direct relationship between these structures in emotional perception. Moreover, studies in which ventral prefrontal regions are rapidly sampled with sufficient signal quality may provide additional information relevant to both dorsal and ventral networks during emotional picture perception (Bechara, 2004; Morrison and Salzman, 2011).

The GC analysis of the interaction between FEF and IPS identified significantly greater directional connectivity from IPS to FEF than the reverse, an effect possibly realized via the inferior fronto-occipital fasciculus (Wakana et al., 2004). This result is distinct from prior investigations of this network in preparatory visuospatial attention tasks (Grent-t-Jong and Woldorff, 2007; Bressler et al., 2008) in which participants were asked to maintain central fixation and anticipate the onset of weak, peripherally-presented target stimuli. In the current experiment, the foveally-presented complex emotional and neutral scene stimuli may have led to a pattern of directional connectivity in which IPS informs FEF to a greater extent than the reverse. An electrocortical study in which steady-state visual-evoked potentials recorded during emotional and neutral picture perception were analyzed using GC suggests that directive connectivity may exist from superior parietal to inferior temporal, and anterior temporal to dorsal prefrontal regions (Keil et al., 2009), and thus future studies employing rapidly sampled BOLD signal may investigate the directional connectivity across subcortical and prefrontal, as well as ventral and dorsal visual attention regions.

STUDY LIMITATIONS

Our primary goal in this experiment was to determine if the emotional discrimination we knew to exist in the FP network preceded such discrimination in the amygdala and FG. While it may be tempting to interpret the relative timing of emotional discrimination as suggesting a hierarchy from ventral to dorsal structures, the current data cannot speak of this relationship directly, as these regions were sampled at different times. Moreover, GC analyses were performed to address separate questions relevant to the processes of emotional perception within dorsal and ventral networks. Again, these data cannot speak of the direct causal relationships between dorsal and ventral structures, as these regions were sampled

independently. We hope that future work will begin to define a direct relationship between the dorsal and ventral structures. Despite these apparent limitations, we believe the current study to be a critical and necessary step in this line of investigation that offers unique and considerable value through innovative use of available imaging methodology.

Regarding the potentially controversial use of GC analyses with fMRI data, we are confident that as long as hemodynamic responses across regions are not highly variable, the application of GC to BOLD time series data is justified. Accumulating evidence (Bressler et al., 2008; Wen et al., 2012; Sathian et al., 2013) demonstrates the effectiveness of using GC to characterize brain interactions from fMRI data. Moreover, a recent article by Wen and colleagues focused on this issue (Wen et al., 2013) concluded that GC is a practical technique for fMRI data analysis. Here, in our data, the hemodynamic latency variability was low (see Fig. 6), and the sampling interval was much faster than is typically used, providing greater characterization of BOLD contrast. We also note that we collected relatively few trials per subject, and this may impact the reliability of our analyses. As a result of hardware constraints on our MR scanner, we were limited to 4096 successive image samples, and this practical concern limited the number of trials that could be collected per block at our fast sampling rate. Thus our Granger analyses were conducted with 20 experimental trials per region in each participant. However, other design factors (large N , many data points per trial epoch) enabled the total number of data points used in our Granger analyses to remain high, and equivalent to prior investigations of fMRI data with GC (Bressler et al., 2008). Thus, we feel confident that our data collection scheme and analyses support our inferences.

Our emotional picture paradigm is comparatively direct, as subjects are simply asked to attend to each 2-s picture and maintain fixation. While this low-load task has been considered to foster variability in hemodynamic data (Specht et al., 2003), we believe the basic nature of the task to be an empirical strength that highlights the dynamic neural mechanisms engaged in the moments directly after picture onset. This basic perceptual-attentive process is thus differentially driven (across trials) most essentially by the content of the picture itself, and not by competing tasks that exist prior to or in concert with stimulus onset. Of course these are empirical questions that may be investigated in future studies employing within-subject single- and dual-task designs.

In summary, here we sought to determine whether the emotionally-enhanced BOLD signal in the ventral visual cortex might be driven by scene-processing mechanisms within the FP visual attention network, by examining the latency of emotionally-enhanced BOLD signal in the dorsal and ventral regions of interest using rapid functional imaging while a gender-balanced sample of 42 participants viewed a balanced set of emotional and neutral scenes. We replicated the timing of the emotionally-enhanced BOLD signal within the amygdala and FG to between 2 and 3 s after stimulus

onset (Sabatinelli et al., 2009), and found latencies between 4 and 5 s in FEF and IPS. Consistent with a reentrant perspective of emotional scene perception, significantly greater directional connectivity was evident from the amygdala to FG than the reverse, while IPS showed greater directional connectivity to FEF than the reverse in this emotional scene-viewing paradigm. These data suggest that emotionally-enhanced activity in human ventral visual structures is not driven by discrimination processes in dorsal visual attention networks, and may instead reflect feedback from the subcortical amygdala, or other structures such as ventral prefrontal regions that may be sampled in future studies.

CONFLICT OF INTEREST

The authors declare no competing financial interests.

REFERENCES

- Adhikari BM, Sathian K, Epstein CM, Lamichhane B, Dhamala M (2014) Oscillatory activity in neocortical networks during tactile discrimination near the limit of spatial acuity. *Neuroimage* 91:300–310.
- Adolphs R (2002) Neural systems for recognizing emotion. *Curr Opin Neurobiol* 12:169–177.
- Aguirre G, Zarahn E, D'Esposito M (1998) The variability of human, BOLD hemodynamic responses. *Neuroimage* 8:360–369.
- Anderson AK, Phelps EA (2001) Lesions of the human amygdala impair enhanced perception of emotionally salient events. *Nature* 411:305–309.
- Anticevic A, Repovs G, Corlett PR, Barch DM (2011) Negative and nonemotional interference with visual working memory in schizophrenia. *Biol Psychiatry* 70:1159–1168.
- Antzoulatos EG, Miller EK (2014) Increases in Functional Connectivity between Prefrontal Cortex and Striatum during Category Learning. *Neuron* 83:216–225.
- Armory JL, Dolan RJ (2002) Modulation of spatial attention by fear-conditioned stimuli: an event-related fMRI study. *Neuropsychologia* 40:817–826.
- Armstrong KM, Chang MH, Moore T (2009) Selection and maintenance of spatial information by frontal eye field neurons. *J Neurosci* 29:15621–15629.
- Asplund CL, Todd JJ, Snyder AP, Marois R (2010) A central role for the lateral prefrontal cortex in goal-directed and stimulus-driven attention. *Nat Neurosci* 13: 507–U136.
- Bechara A (2004) The role of emotion in decision-making: evidence from neurological patients with orbitofrontal damage. *Brain Cogn* 55:30–40.
- Bisley JW, Goldberg ME (2010) Attention, intention, and priority in the parietal lobe. *Annu Rev Neurosci* 33:1–21.
- Bressler SL, Tang W, Sylvester CM, Shulman GL, Corbetta M (2008) Top-down control of human visual cortex by frontal and parietal cortex in anticipatory visual spatial attention. *J Neurosci* 28:10056–10061.
- Brosch T, Grandjean D (2013) Cross-modal modulation of spatial attention by emotion. Integrating face and voice in person perception. Springer. p. 207–223.
- Buxton RB, Wong EC, Frank LR (1998) Dynamics of blood flow and oxygenation changes during brain activation: the balloon model. *Magn Reson Med* 39:855–864.
- Carrette L (2014) Exogenous (automatic) attention to emotional stimuli: a review. *Cogn Affect Behav Neurosci* 1–31.
- Catani M, Jones DK, Donato R (2003) Occipito-temporal connections in the human brain. *Brain* 126:2093.
- Codispoti M, Ferrari V, Bradley MM (2006) Repetitive picture processing: autonomic and cortical correlates. *Brain Res* 1068:213–220.
- Corbetta M (1998) Frontoparietal cortical networks for directing attention and the eye to visual locations: identical, independent, or overlapping neural systems? *Proc Natl Acad Sci USA* 95:831–838.
- Corbetta M, Shulman GL (2002) Control of goal-directed and stimulus-driven attention in the brain. *Nat Rev Neurosci* 3:201–215.
- Corbetta M, Patel G, Shulman GL (2008) The reorienting system of the human brain: from environment to theory of mind. *Neuron* 58:306–324.
- Dhamala M, Rangarajan G, Ding M (2008) Analyzing information flow in brain networks with nonparametric Granger causality. *Neuroimage* 41:354–362.
- Ding M, Chen Y, Bressler SL (2006) Granger causality: basic theory and application to neuroscience. In: Schelter B, Winderhalder M, Timmer J, editors. *Handbook of time series analysis*. Berlin: Wiley-VCH. p. 437–460.
- Dyckman KA, Camchong J, Clementz BA, McDowell JE (2007) An effect of context on saccade-related behavior and brain activity. *Neuroimage* 36:774–784.
- Feinberg DA, Setsompop K (2013) Ultra-fast MRI of the human brain with simultaneous multi-slice imaging. *J Magn Res* 229:90–100.
- Ferri F, Ebisch SJ, Costantini M, Salone A, Arciero G, Mazzola V, Ferro FM, Romani GL, Gallese V (2013) Binding action and emotion in social understanding. *PLoS One* 8:e54091.
- Frank DW, Sabatinelli D (2012) Stimulus-driven reorienting in the ventral frontoparietal attention network: the role of emotional content. *Front Human Neurosci* 6.
- Freese JL, Amaral DG (2005) The organization of projections from the amygdala to visual cortical areas TE and V1 in the macaque monkey. *J Comp Neurol* 486:295–317.
- Friston KJ, Fletcher P, Josephs O, Holmes A, Rugg MD, Turner R (1998) Event-related fMRI: characterizing differential responses. *Neuroimage* 7(1):30–40.
- Genovese CR, Lazar NA, Nichols T (2002) Thresholding of statistical maps in functional neuroimaging using the false discovery rate. *Neuroimage* 15:870–878.
- Geweke J (1982) Measurement of linear dependence and feedback between multiple time series. *J Am Stat Assoc* 77:304–313.
- Grent-t-Jong T, Woldorff MG (2007) Timing and sequence of brain activity in top-down control of visual-spatial attention. *PLoS Biol* 5:e12.
- Grill-Spector K, Malach R (2004) The human visual cortex. *Annu Rev Neurosci* 27:649–677.
- Hegde J, Felleman DJ (2007) Reappraising the functional implications of the primate visual anatomical hierarchy. *Neuroscientist* 13:416–421.
- Junghöfer M, Bradley MM, Elbert TR, Lang PJ (2001) Fleeting images: a new look at early emotion discrimination. *Psychophysiology* 38:175–178.
- Keil A, Sabatinelli D, Ding M, Lang PJ, Ihssen N, Heim S (2009) Reentrant projections modulate visual cortex in affective perception: evidence from Granger causality analysis. *Hum Brain Mapp* 30:532–540.
- Kim SG, Richter W, Uğurbil K (1997) Limitations of temporal resolution in functional MRI. *Magn Reson Med* 37:631–636.
- Kirchner H, Barbeau EJ, Thorpe SJ, Regis J, Liegeois-Chauvel C (2009) Ultra-rapid sensory responses in the human frontal eye field region. *J Neurosci* 29:7599–7606.
- Lamme VA, Roelfsema PR (2000) The distinct modes of vision offered by feedforward and recurrent processing. *Trends Neurosci* 23:571–579.
- Lang PJ, Bradley MM (2010) Emotion and the motivational brain. *Biol Psychol* 84:437–450.
- Lang PJ, Bradley MM, Fitzsimmons JR, Cuthbert BN, Scott JD, Moulder B, Nangia V (1998) Emotional arousal and activation of the visual cortex: an fMRI analysis. *Psychophysiology* 35:199–210.
- Lang PJ, Bradley MM, Cuthbert BN (2008) International affective picture system (IAPS): affective ratings of pictures and instruction manual. Technical Report A-8. Gainesville, FL: University of Florida.

- Lin F-H, Witzel T, Raij T, Ahveninen J, Wen-Kai Tsai K, Chu Y-H, Chang W-T, Nummenmaa A, Polimeni JR, Kuo W-J (2013) fMRI hemodynamics accurately reflects neuronal timing in the human brain measured by MEG. *Neuroimage* 78:372–384.
- Liu Y, Huang H, McGinnis-Deweese M, Keil A, Ding M (2012) Neural substrate of the late positive potential in emotional processing. *J Neurosci* 32:14563–14572.
- Logothetis NK, Wandell BA (2004) Interpreting the BOLD signal. *Ann Rev Physiol* 66:735–769.
- Maris E (2004) Randomization tests for ERP topographies and whole spatiotemporal data matrices. *Psychophysiology* 41:142–151.
- Maris E, Oostenveld R (2007) Nonparametric statistical testing of EEG-and MEG-data. *J Neurosci Methods* 164:177–190.
- Markovic J, Anderson AK, Todd RM (2013) Tuning to the significant: neural and genetic processes underlying affective enhancement of visual perception and memory. *Behav Brain Res* 259C:229–241.
- Menon RS, Kim S-G (1999) Spatial and temporal limits in cognitive neuroimaging with fMRI. *Trends Cogn Sci* 3:207–216.
- Miezin FM, Maccotta L, Ollinger J, Petersen S, Buckner R (2000) Characterizing the hemodynamic response: effects of presentation rate, sampling procedure, and the possibility of ordering brain activity based on relative timing. *Neuroimage* 11:735–759.
- Mitchell DG, Luo Q, Mondillo K, Vythilingam M, Finger EC, Blair RJ (2008) The interference of operant task performance by emotional distracters: an antagonistic relationship between the amygdala and frontoparietal cortices. *Neuroimage* 40:859–868.
- Moratti S, Keil A, Stolarova M (2004) Motivated attention in emotional picture processing is reflected by activity in cortical attention networks. *Neuroimage* 21:945–964.
- Morrison SE, Salzman CD (2011) Representations of appetitive and aversive information in the primate orbitofrontal cortex. *Ann N Y Acad Sci* 1239:59–70.
- Nakamura K, Matsumoto K, Mikami A, Kubota K (1994) Visual response properties of single neurons in the temporal pole of behaving monkeys. *J Neurophysiol* 71:1206–1221.
- Nishijo H, Hori E, Tazumi T, Ono T (2008) Neural correlates to both emotion and cognitive functions in the monkey amygdala. *Behav Brain Res* 188:14–23.
- Paus T (1996) Location and function of the human frontal eye-field: a selective review. *Neuropsychologia* 34:475–483.
- Pessoa L, Adolphs R (2010) Emotion processing and the amygdala: from a 'low road' to 'many roads' of evaluating biological significance. *Nat Rev Neurosci* 11:773–783.
- Pessoa L, Japee S, Sturman D, Ungerleider LG (2006) Target visibility and visual awareness modulate amygdala responses to fearful faces. *Cereb Cortex* 16:366–375.
- Pourtois G, Grandjean D, Sander D, Vuilleumier P (2004) Electrophysiological correlates of rapid spatial orienting towards fearful faces. *Cereb Cortex* 14:619–633.
- Rizzolatti G, Riggio L, Dascola I, Umiltà C (1987) Reorienting attention across the horizontal and vertical meridians: evidence in favor of a premotor theory of attention. *Neuropsychologia* 25:31–40.
- Sabatinelli D, Bradley MM, Fitzsimmons JR, Lang PJ (2005) Parallel amygdala and inferotemporal activation reflect emotional intensity and fear relevance. *Neuroimage* 24:1265–1270.
- Sabatinelli D, Bradley MM, Lang PJ, Costa VD, Versace F (2007a) Pleasure rather than salience activates human nucleus accumbens and medial prefrontal cortex. *J Neurophysiol* 98:1374–1379.
- Sabatinelli D, Lang PJ, Keil A, Bradley MM (2007b) Emotional perception: correlation of functional MRI and event-related potentials. *Cereb Cortex* 17:1085–1091.
- Sabatinelli D, Fortune EE, Li Q, Siddiqui A, Krafft C, Oliver WT, Beck S, Jeffries J (2011) Emotional perception: meta-analyses of face and natural scene processing. *Neuroimage* 54:2524–2533.
- Sabatinelli D, Lang PJ, Bradley MM, Costa VD, Keil A (2009) The timing of emotional discrimination in human amygdala and ventral visual cortex. *J Neurosci* 29:14864–14868.
- Sabatinelli D, Keil A, Frank DW, Lang PJ (2013) Emotional perception: correspondence of early and late event-related potentials with cortical and subcortical functional MRI. *Biol Psychol* 92:513–519.
- Sathian K, Deshpande G, Stilla R (2013) Neural changes with tactile learning reflect decision-level reweighting of perceptual readout. *J Neurosci* 33(12):5387–5398.
- Schafer RJ, Moore T (2007) Attention governs action in the primate frontal eye field. *Neuron* 56:541–551.
- Schmolsky MT, Wang Y, Hanes DP, Thompson KG, Leutgeb S, Schall JD, Leventhal AG (1998) Signal timing across the macaque visual system. *J Neurophysiol* 79:3272–3278.
- Serences JT, Yantis S (2006) Selective visual attention and perceptual coherence. *Trends Cogn Sci* 10:38–45.
- Shafer AT, Dolcos F (2012) Neural correlates of opposing effects of emotional distraction on perception and episodic memory: an event-related fMRI investigation. *Front Integr Neurosci* 6:70.
- Specht K, Willmes K, Shah NJ, Jaencke L (2003) Assessment of reliability in functional imaging studies. *J Magn Res Imag* 17:463–471.
- Sugase Y, Yamane S, Ueno S, Kawano K (1999) Global and fine information coded by single neurons in the temporal visual cortex. *Nature* 400:869–873.
- Talairach J, Tournoux P (1988) Co-planar stereotaxic atlas of the human brain. New York: Georg Thieme.
- Taylor PC, Nobre AC, Rushworth MF (2007) FEF TMS affects visual cortical activity. *Cereb Cortex* 17:391–399.
- Thompson KG, Biscoe KL, Sato TR (2005) Neuronal basis of covert spatial attention in the frontal eye field. *J Neurosci* 25:9479–9487.
- Tsuchiya N, Moradi F, Felsen C, Yamazaki M, Adolphs R (2009) Intact rapid detection of fearful faces in the absence of the amygdala. *Nat Neurosci* 12:1224–1225.
- Vanrullen R, Thorpe SJ (2001) The time course of visual processing: from early perception to decision-making. *J Cogn Neurosci* 13:454–461.
- Vuilleumier P, Driver J (2007) Modulation of visual processing by attention and emotion: windows on causal interactions between human brain regions. *Philos Trans R Soc Lond B Biol Sci* 362:837–855.
- Vuilleumier P, Huang YM (2009) Emotional attention: uncovering the mechanisms of affective biases in perception. *Curr Direct Psychol Sci* 18:148–152.
- Vuilleumier P, Richardson MP, Armony JL, Driver J, Dolan RJ (2004) Distant influences of amygdala lesion on visual cortical activation during emotional face processing. *Nat Neurosci* 7:1271–1278.
- Vuilleumier P, Schwartz S, Duhoux S, Dolan RJ, Driver J (2005) Selective attention modulates neural substrates of repetition priming and "implicit" visual memory: suppressions and enhancements revealed by fMRI. *J Cogn Neurosci* 17:1245–1260.
- Wakana S, Jiang H, Nagae-Poetscher LM, Van Zijl PC, Mori S (2004) Fiber tract-based atlas of human white matter anatomy. *Radiology* 230:77–87.
- Wen X, Yao L, Liu Y, Ding M (2012) Causal interactions in attention networks predict behavioral performance. *J Neurosci* 32:1284–1292.
- Wen X, Rangarajan G, Ding M (2013) Is Granger causality a viable technique for analyzing fMRI data? *PLoS One* 8(7):e67428.
- Wiens S, Syrjanen E (2013) Directed attention reduces processing of emotional distracters irrespective of valence and arousal level. *Biol Psychol* 94:44–54.